UCRL 3266

J. Coleman

UNIVERSITY OF CALIFORNIA

Radiation Laboratory

FISSION AND SPALLATION EXCITATION FUNCTIONS OF U^{238}

TWO-WEEK LOAN COPY

This is a Library Circulating Copy which may be borrowed for two weeks. For a personal retention copy, call Tech. Info. Division, Ext. 5545

UCRL-3266
Chemistry distribution

UNIVERSITY OF CALIFORNIA

Radiation Laboratory
Berkeley, California

Contract No. W-7405-eng-48

FISSION AND SPALLATION EXCITATION FUNCTIONS OF U^{238}

Susanne Elaine Ritsema
(Master's Thesis)

January 20, 1956

Printed for the U. S. Atomic Energy Commission

FISSION AND SPALLATION EXCITATION FUNCTIONS OF U^{238}

Contents

Abstract 3
I. Introduction 4
II. Experimental Procedures 6
A. Target Assembly 6
B. Target Preparation 7
C. Chemical Procedures 8
D. Mounting of Samples 14
E. Counting Instruments 15
III. Treatment of Data 16
A. Yield Determination 16
B. Isotope Identification 16
C. Decay Curve Resolution 16
D. Calculation of Disintegrations per Minute 17
E. Corrections for Conversion Electrons 21
F. Parent-Daughter Relationships 21
G. Cross-Section Calculations 21
IV. Results 23
A. Spallation Cross Sections 23
B. Fission Product Cross Sections 23
V. Discussion 27
A. Spallation Reactions 28
B. Fission Yields 29
Acknowledgments 31
References 33

FISSION AND SPALLATION EXCITATION FUNCTIONS OF U^{238}

Susanne Elaine Ritsema
Radiation Laboratory and Department of Chemistry
University of California, Berkeley, California

January 20, 1956

ABSTRACT

Fission and spallation products produced in 22- to 46-Mev helium-ion bombardments of U^{238} were isolated by chemical methods. Various isotopes were identified by their radioactive properties. Absolute fission and spallation cross sections were determined at various energies and plotted as a function of energy. The (α, p2n) reaction was observed below the threshold for evaporation of a proton and two neutrons and, therefore, it was concluded that tritium emission is occurring. The (α, αn) product was the most prominent spallation product observed. Fission yield curves show an increase of symmetry with energy, and the minimum in the fission yield curve vanishes at 40 Mev.

FISSION AND SPALLATION EXCITATION FUNCTIONS OF U^{238}

Susanne Elaine Ritsema
Radiation Laboratory and Department of Chemistry
University of California, Berkeley, California

January 20, 1956

I. INTRODUCTION

This work is a radiochemical investigation of the energy dependence of the cross section for formation of certain nuclides produced in the bombardment of U^{238} with helium ions. The helium ion energies ranged from 22 to 46 Mev.

The reactions that helium ions undergo with heavy nuclei are inelastic scattering, elastic scattering, spallation, and fission. In both scattering processes the target and product nuclei have the same mass and atomic number. Spallation reactions involve the emission of small particles such as neutrons, protons, tritons, and alpha particles from the bombarded nuclide. In fission reactions, the nucleus splits into two large fragments in addition to emitting neutrons. The prominence of the various reactions depends upon the energy of the bombarding helium ions. Of these types of reactions, only spallation and fission can be studied by use of radiochemical methods.

Fission reactions of many nuclides have been observed.[1] The ease with which a nuclide fissions seems to be related to Z^2/A of the target nucleus.[2] With increasing Z^2/A the energy requirements for fission are lowered. Thus, fission can be induced by 1-Mev neutrons[3] in U^{238}, but requires about 300-Mev protons for tantalum.[4] In general, fission becomes more prominent and spallation less prominent with increasing atomic number. Marked differences have been observed between fission reactions induced by low-energy projectiles and those induced by high-energy projectiles. Low-energy fission is asymmetric; e.g., in 1-Mev neutron-induced fission of U^{238} the most probable fragments[3] have masses of 98 and 138. Also, the primary fission fragments have a neutron excess and are all beta-particle emitters. The liquid-drop model[2] is useful in describing certain features of the mechanism of low-energy fission. This model has not been successful in explaining

the asymmetry of low-energy fission. High-energy fission (>100 Mev) is symmetric, and the primary fission fragments have a lower neutron-to-proton ratio than in asymmetric fission. The mechanism proposed by Goeckermann and Perlman[5] for 190-Mev deuteron-induced fission of Bi^{209} includes the concept of prefission evaporation of 10 to 12 neutrons. Their experimental evidence supports the hypothesis that in this case there are only two or three fissioning nuclides. Results of high-energy bombardments of uranium[6] indicate that some prefission evaporation of neutrons is taking place, but in this case the fission products seem to be formed from several fissioning nuclides. Thus the mechanism of fission seems to vary both with the energy of the bombarding particle and with the mass of the target. The fission reactions of U^{238} studied in this work are of particular interest because previous experiments[7-10] have shown that fission symmetry changes rapidly in this energy region (22 to 46 Mev). Turkevich[11] has suggested that both symmetric and asymmetric processes are occurring at intermediate energies.

The mechanism of spallation reactions induced by low-energy particles (<50 Mev) is usually described by the compound nucleus theory. This theory postulates that the projectile is absorbed by the target nucleus and that its energy is rapidly shared with the other nucleons. After many energy exchanges enough energy is concentrated on one particle so that it can be emitted. The number of particles that can be emitted increases with projectile energy. The method of deexcitation of the compound nucleus should depend on its excitation energy, angular momentum, and parity, but not otherwise on the specific way in which it has been formed.[12] Ghoshal[13] tested this hypothesis by bomarding Cu^{63} with protons and Ni^{60} with helium ions. Comparison of their excitation functions shows agreement with the compound-nucleus theory. The following experimental results of other reactions, indicate, however, that compound-nucleus formation may not be taking place:

1. The angular distribution of neutrons produced in (p, n) reactions is strongly peaked forward.[14]
2. Nuclear temperatures predicted by the theory do not agree with those determined experimentally.[15-17]
3. Proton-emission cross sections are much higher than predicted.[18-21] For example, the ratio of the observed to the calculated Pb^{208} (n, p) Tl^{208} cross sections is 16,000.[18]

The compound-nucleus theory postulates that proton emission is much less probable than neutron emission from high-Z targets because coulombic repulsion tends to keep protons inside the nucleus. However, if some low-energy projectiles are interacting directly with target nucleons instead of forming a compound nucleus, the probability of proton emission is greater.[22] This direct-interaction mechanism is typical of high-energy spallation reactions.[23] The magnitude of the (α, pxn) cross section of U^{238} should indicate whether or not some direct interaction of low-energy helium ions (<50 Mev) with nucleons may be taking place. The work reported here is part of a series of studies of medium-energy fission and spallation reactions of heavy nuclei with helium ions, deuterons, and protons. It is hoped that systematic trends will be revealed in the variation of the magnitude of fission and spallation cross sections with mass, atomic number, and nuclear type (odd-odd, even-odd, and even-even). The first experimental study of this series--namely, Pu^{239} bombarded with helium ions,[10] --has been completed. In this work, cross sections of the (α, 4n), (α, pn), (α, p2n), (α, p3n), α, αn), and (α, fission) reactions of U^{238} were determined at several energies ranging from 22 to 46 Mev.

The following section presents the experimental procedures used in the bombardments. In the third section, treatment of data is discussed with special attention given to evaluation of counting corrections. Results are presented in tables and graphs in the fourth section and the results are discussed in the final section.

II. EXPERIMENTAL PROCEDURES

A. Target Assembly

The target assembly used in most bombardments was similar to that used by Glass in the Pu^{239} bombardments.[10] The external 48-Mev helium ion beam of the Crocker Laboratory 60-in cyclotron was degraded to the desired energy by aluminum and platinum foils. The foils were placed in an air-cooled block in front of the water-cooled pistol-grip target holder. Aluminum degrading foils do not burn out nearly as often as platinum and, therefore, are more satisfactory. The number of helium ions bombarding the target was determined by measuring the target current. Beam integrators

recorded the total beam hitting the target. Beam patterns were taken before each bombardment to make certain that all of the collimated beam was striking the target.

A new type of target assembly called the microtarget assembly was used in the bombardments at 23, 43, and 46 Mev. The advantages of this microtarget are that it offers better cooling and is easier to assemble than the pistol-grip assembly. The microtarget assembly is illustrated in Fig. 1.

Since the energy of the helium ions striking the target depends on the thickness and kind of degrading foils used, the foils were always measured and weighed. The energy was calculated from range-energy data.[24]

A 1-mil aluminum foil was always placed on top of the target in order to catch the fission recoils. This foil was dissolved along with the target.

B. Target Preparation

In order to calculate absolute cross sections in the case wherein all of the beam hits the target, the number of atoms per square centimeter of target material must be known. Since this requires a uniform deposit, the electrodeposition method developed by Hufford and Scott[25] was used.

A concentrated nitric acid solution containing isotopically pure (>99.9 percent) U^{238} was boiled to dryness. This was dissolved in 0.4 M ammonium oxalate and the resulting solution transferred to a plating cell. The uranium (as the hydrous oxide) was deposited uniformly over approximately 1 cm^2 of a 10-mil aluminum hat-shaped foil. It was found that 0.2 mg to one mg of uranium could be electroplated in 15 min if a current of 100 ma was maintained at 4 v between a platinum stirring disk (anode) and the aluminum "hat" (cathode).

Two methods were used to determine the amount of uranium deposited. The aluminum hat was weighed before and after plating, and the target was counted in an alpha ionization chamber. The weight occasionally failed to check with the amount of uranium determined by alpha counting. In this case several checks were made using several alpha counters and the alpha pulse analyzer. The count values always agreed and, therefore, these data were considered to be more accurate than weight data. To convert the alpha counting rate of U^{238} to mg U^{238}, the specific activity value of 739.9 disintegrations per mg of U^{238} was used.[26]

C. Chemical Procedures

In order to study the fission and spallation reactions of U^{238}, several fission products and actinide elements were isolated by radiochemical methods. Uranium, neptunium, and plutonium fractions were isolated in nearly every experiment and various fission products were isolated in several experiments. Np^{237} and Pu^{239} were added to the target solutions as tracers so that yield could be determined accurately. The U^{238} target material served as tracer for the uranium fraction. In these bombardments (2 to 18 microampere-hours) the activities of the fission products were low, and therefore, the products were separated in a series of steps from the entire target instead of being separated as aliquots. Those fission products which would not interfere with isolation of the spallation products were selected, and known amounts of inactive carrier ranging from 10 to 30 mg were added to the target solution for each fission product isolated.

The chemical procedures used with the bombardments at 25.2, 27.1, and 32.5 Mev differ from the improved procedures used with the other later bombardments.

1. First Chemical Procedures.

Zirconium, cadmium, and cerium carriers were added to the target solution in addition to the Np^{237} and Pu^{239} tracers. The target was dissolved in nitric and hydrochloric acids. Sodium hydroxide was then added and zirconium, cerium, neptunium, uranium, and plutonium were precipitated as the hydroxides. Cadmium and aluminum remained in solution. The precipitate was dissolved in hydrochloric acid and cerous fluoride was precipitated by the addition of hydrofluoric acid. The cerium fluoride precipitate carried neptunium and plutonium, leaving uranium and zirconium in the supernatant solution. The fluoride precipitate was dissolved in a mixture of 6M nitric acid and saturated boric acid and then another hydroxide was precipitated with ammonium hydroxide. The precipitate was dissolved in hydrochloric acid and the solution saturated with hydrogen chloride gas. This solution was passed through a (3mm x 2.5 cm) glass column packed with Dowex A-1 anion exchange resin. The rare earth elements pass through the resin bed, but neptunium and plutonium are absorbed. To ensure separation of neptunium and plutonium from rare earths, the resin was washed with two column volumes of concentrated hydrochloric acid. Neptunium and plutonium were then stripped

from the resin with 1 N hydrochloric acid. The solution containing the neptunium and plutonium was adjusted to 1 M hydrochloric acid and 0.005 M hydrazine dihydrochloride, and was heated in order to reduce plutonium to the (III) state and neptunium to the (IV) state. The solution was cooled, saturated with hydrogen chloride gas, and passed through a second column packed with Dowex-A-1 anion-exchange resin. Neptunium and plutonium are separated in this step; neptunium is absorbed by the resin, but plutonium passes through the column. The resin was washed with several column volumes of a solution 0.1 M hydriodic acid and concentrated hydrochloric acid in order to remove all traces of plutonium. The isolated plutonium was then prepared for counting. The neptunium was desorbed from the column with 1 M hydrochloric acid and extracted into a TTA (thenoyltrifluoracetone) solution, as described below in the improved procedure.

Zirconium was precipitated as barium fluozirconate from the fluoride supernatant solution by adding barium chloride. Uranium remained in the supernatant solution. Boric acid crystals were added to the supernatant solution, complexing the fluoride ion present. Addition of lanthanum and ammonium hydroxide resulted in the precipitation of lanthanum hydroxide, which carried uranium. The precipitate was digested in a saturated sodium carbonate solution. Uranium formed a soluble carbonate complex. The solution was separated from the precipitate, acidified, and boiled in order to remove carbonate. The final purification procedure consisted of saturating the solution with hydrogen chloride gas, passing it through a glass column packed with Dowex A-1 anion-exchange resin, which absorbed the uranium, washing the resin with 6 M HCl, and stripping off the uranium with 0.1 M HCl.

The disadvantages of this chemical procedure are:

(a) The yields of neptunium and uranium are low.

(b) The neptunium procedure takes too long. The half-life of Np^{241} was reported to be 15 min.[28] There is no chance of observing such a short-lived activity with this procedure.

(c) The yields of fission products, especially cerium and cadmium, are low.

2. Improved Chemical Procedure.

Target Dissolution. Ruthenium, cadmium, cerium, barium, strontium, and zirconium carriers, in addition to Np^{237} and Pu^{239} traces, were added to the target solution. The target was dissolved in concentrated hydrochloric

acid. The ruthenium metal that precipitated from the solution was centrifuged off.

Neptunium. The target solution was adjusted so that the concentration of ferrous ion was 0.005 M and hydrazine dihydrochloride was 0.1 M, and was heated five minutes at 50° C in order to reduce neptunium to the (IV) state and plutonium to the (III) state. This solution was made 0.05 M in orthophosphoric acid, precipitating zirconium phosphate, which carries neptunium. Uranium, plutonium, the rare earths, barium, strontium, and cadmium remained in the supernatant solution. The zirconium phosphate precipitate was dissolved in a solution containing a mixture of hydrofluoric acid and nitric acid. Lanthanum nitrate solution was added and lanthanum fluoride formed, which carries neptunium. (The steps listed thus far are slight modifications of the neptunium separation procedure developed by Magnusson et al.)[29] The lanthanum fluoride precipitate was dissolved in a 6 M HNO_3 solution saturated with boric acid. Lanthanum hydroxide was then precipitated as a result of the addition of ammonium hydroxide, the precipitate carrying neptunium. The precipitate was dissolved in hydrochloric acid, the solution adjusted to 1 M hydrochloric acid, 0.2 M hydroxylamine dihydrochloride and heated for one min. The solution was adjusted to 1 M postassium iodide, a few drops of stannous chloride were added, and the solution was heated again. The purpose of these steps was to ensure reduction of neptunium to the (IV) state and traces of plutonium present to the (III) state. After the solution was cooled, neptunium was extracted from it with an equal volume of 0.4 M TAA in benzene. Neptunium was then reextracted with 12 M HCl.

Plutonium. The supernatant solution remaining from the zirconium phosphate precipitation step was adjusted to 0.1 M sodium bromate and heated for one min to oxidize plutonium from the (III) state to the (IV) state. Addition of zirconium resulted in the precipitation of zirconium phosphate, which carried the plutonium. The precipitate was dissolved in hydrofluoric and nitric acids. Lanthanum nitrate solution was added and the lanthanum fluoride precipitate formed carried the plutonium. The lanthanum fluoride precipitate was dissolved in nitric acid and boric acid, and lanthanum was precipitated as the hydroxide by addition of ammonium hydroxide to the solution. The precipitate was dissolved in hydrochloric acid, and the solution was saturated with hydrogen chloride gas and passed through a column packed with Dowex A-1 anion exchange resin, which absorbed plutonium. The final purification steps consisted

of washing the resin with several column volumes of concentrated hydrochloric acid and finally desorbing plutonium from the resin with a solution of 12 M hydrochloric acid and 0.1 M hydriodic acid.

Uranium (Procedure I). The procedure used to isolate uranium depended on the energy of the bombardment. At energies above 34 Mev, it was possible for the (α, 2pn) product, U^{239}, which has a 23-min half-life to be formed, and a fast chemical procedure was necessary. In this case, a small (approximately 15 percent) aliquot of the target solution was adjusted to 8 M HCl and passed through a column packed with Dowex A-1 anion-exchange resin, which absorbed neptunium, plutonium, and uranium. After the resin had been washed, the actinide elements were desorbed with 1 M HCl. Hydroxylamine was added in order to reduce neptunium and plutonium below the (VI) state. Addition of lanthanum and ammonium hydroxide precipitated lanthanum hydroxide, which carried neptunium, plutonium, and uranium. The precipitate was dissolved in nitric acid and the solution saturated with ammonium nitrate. The solution was equilibrated with diethyl ether, which extracted uranium that was in the (VI) state, but not neptunium and plutonium, since these were in lower oxidation states. The ether phase was washed with 10 M ammonium nitrate and the uranium was then reextracted into water. Four extraction cycles were required to give an appreciable yield. The water was boiled to remove ether, saturated with hydrogen chloride gas, and passed through another column packed with Dowex A-1 anion-exchange resin. The resin was washed with hydrochloric acid, and the uranium stripped off with 1 M hydrochloric acid. The purpose of this final step was to remove the salts that had reextracted with uranium from the ether phase.

Uranium (Procedure II). In bombardments below 34 Mev, the 23-min U^{239} activity could not be produced and, therefore, a more lengthy procedure was used, since better yield could be obtained in this way. The uranium was separated from the supernatant solution from the second zirconium phosphate precipitation. This solution was made basic with sodium hydroxide, and 2 ml sodium carbonate was added. This resulted in precipitation of barium, strontium, the rare earths, and uranium. Cadmium remained in solution. The precipitate was dissolved in hydrochloric acid, and barium and strontium chlorides were precipitated by saturating the solution with hydrogen chloride gas. The supernatant solution was passed through a column packed with Dowex A-1 anion-exchange resin, which absorbed uranium but not the rare

earths. The uranium was stripped from the column with 1 M hydrochloric acid. The final purification steps consisted of ether extraction and another anion-column step as described in the fast uranium chemical procedure.

3. Fission-Product Chemical Procedures.

The fission product isolation procedures are modifications of procedures listed by Meinke,[30] Coryell and Sugarman,[31] and Lindner.[32]

Ruthenium. The ruthenium metal that had precipitated in the target-dissolution step was dissolved by heating in the presence of concentrated nitric and hydrochloric acids. The solution was placed in a distilling flask; sodium bismuthate, perchloric acid, orthophosphoric acid, and sodium iodide were added, the mixture was heated, and ruthenium tetraoxide was distilled off into a 6 M NaOH solution. Addition of ethyl alcohol to the solution precipitated ruthenium dioxide. The precipitate was dissolved in hydrochloric acid and magnesium metal was added in order to reduce ruthenium dioxide to ruthenium metal. Ruthenium metal was then mounted for counting.

Cadmium. The supernatant solution from the sodium hydroxide precipitation of the rare earths, barium, strontium, and uranium was saturated with hydrogen sulfide gas. The precipitate formed was always black, owing to the presence of some ferrous sulfide. This precipitate was dissolved in hydrochloric acid, and the solution was saturated with hydrogen chloride gas and passed through a column packed with Dowex A-1 anion-exchange resin, which absorbed cadmium and iron. The resin was washed with 1 M hydrochloric acid in order to remove iron. Cadmium was eluted from the column with 0.75 M H_2SO_4. The solution was diluted to 0.5 M acid, and yellow cadmium sulfide was precipitated by passing hydrogen sulfide into the solution. The precipitate was dissolved in hydrochloric acid and an antimony sulfide scavenge precipitation was made from a 4 M hydrochloric acid solution. The supernatant was adjusted to 0.5 N HCl and a final precipitation of cadmium sulfide was done.

Barium. The barium and strontium chlorides (uranium procedure) were dissolved in water and then reprecipitated as chlorides. This step separated barium and strontium from the aluminum that had previously precipitated together with the barium and strontium from a solution in which the salt concentration was very high. The precipitate was redissolved in water and the solution buffered to a pH of 5. Barium chromate was then precipitated, with strontium remaining in solution. Sodium carbonate was added to the precipitate to

metathesize it to barium carbonate. A strontium holdback agent was added and barium chromate was then reprecipitated. The barium chromate was mounted, weighed, and counted.

Strontium. The supernatant solution from the barium chromate precipitation step was neutralized and strontium carbonate was precipitated by addition of sodium carbonate. The precipitate was dissolved and reprecipitated in final form as the carbonate after a barium chromate scavenge precipitation step.

Zirconium. Zirconium phosphate was used to carry neptunium. This precipitate was dissolved in nitric and hydrofluoric acid. Addition of lanthanum nitrate solution precipitated lanthanum fluoride, which carried neptunium but left zirconium in solution. (See neptunium procedure.) Addition of barium chloride to this supernatant solution precipitated barium fluozirconate. The precipitate was dissolved in saturated boric and nitric acids and barium was removed from the solution by a barium sulphate precipitation. Zirconium hydroxide was precipitated from the supernatant solution with ammonium hydroxide. The precipitate was dissolved in 1 N HCl and zirconium was extracted from the solution with a solution of 0.4 M TTA in benzene. The TTA phase was washed several times with 6 M HCl and then evaporated in a crucible. This zirconium fraction was ignited to zirconium dioxide and mounted for counting.

Cerium. In bombardments in which cerium was the only rare earth isolated, it was purified by an oxidation-reduction cycle. The cerium that came through the anion-exchange column (uranium procedure) was precipitated as the hydroxide, dissolved in hydrochloric acid, and oxidized to the (IV) state with sodium bromate. Addition of iodic acid precipitated ceric iodate. The precipitate was dissolved in hydrochloric acid and hydrogen peroxide, which reduced cerium to the (III) state. A zirconium iodate scavenge precipitation separated cerium from the other rare earths. Cerium does not form an insoluble iodate in the (III) state, and therefore remained in solution. Cerium was then oxidized to the (IV) state with sodium bromate and ceric iodate was precipitated. Cerium was again dissolved in hydrochloric acid and hydrogen peroxide, and then precipitated successively as the fluoride, hydroxide, and finally as the oxalate.

Other rare earth elements. Several rare earth elements were isolated in bombardments at 27, 38, 40 and 46 Mev. Nervik's method[33] of separating the rare earth element was used. The rare earth elements were precipitated as hydroxides by the addition of ammonium hydroxide, dissolved in hydrochloric acid, and precipitated as the fluorides with hydrofluoric acid. The fluoride precipitate was dissolved in a solution of saturated boric acid in nitric acid. After another hydroxide precipitation, the rare earths were dissolved in hydrochloric acid. The solution was adjusted to 2 M HCl and was equilibrated with 1 cc of Dowex-50 cation resin. This resin was placed on top of a glass column 9 mm by 70 cm, packed with Dowex-50 cation-exchange resin. Since the elution rate of the rare earths depends on the pH of the eluting agent (in addition to other factors), the pH of the lactate eluting agent used was varied continuously from 3 to 5 so that an adequate separation of rare earths in the optimum time might be achieved. Usually the rare earths were separated in one day and showed no sign of contamination. After the rare earths had been eluted, they were precipitated as oxalates, ignited to the oxide, and mounted.

Other fission products. In order to define the shape of the fission yield curve more clearly in an energy region in which the shape is nearly symmetric, a 1-mil U^{238} foil was bombarded with 40-Mev helium ions; palladium, tellurium, silver, and molybdenum, in addition to the previously mentioned fission products, were isolated. Since the aliquot method was used, standard procedures[30, 32] could be followed without modification. No description of these procedures need be included, therefore.

D. Mounting of Samples

1. Actinide Elements.

Neptunium and plutonium samples were prepared for counting by volatilization of the samples from a tantalum filament onto platinum plates. The volatilization was done at a high temperature (>600° C) in an evacuated system. This produced thin samples and good resolution on the alpha pulse analyzer was obtained. Since this method was found to be inefficient for uranium, the uranium samples were evaporated on platinum disks which were then ignited with a Bunsen burner before counting. The decay of neptunium and plutonium was followed on a Nucleometer. The decay of uranium was followed either on the Nucleometer or the Geiger-Müller counter.

2. Fission Products.

The fission products were transferred to weighed aluminum hat-shaped foils, dried under a heat lamp, and weighed in order to determine chemical yield. Sample loss was prevented by coating the sample with zapon immediately after weighing. The decay of fission products was followed on a Geiger-Müller counter.

E. Counting Instruments

1. Alpha Counter.

For gross alpha counting, an argon-filled ionization chamber was used. The counter efficiency is 52 percent for thin samples on platinum backing material.

2. Alpha Pulse Analyzer.

A 48-channel alpha pulse analyzer[34] was used to distinguish between various alpha emitters. It consists of electronic circuits which pick up amplified pulses produced by alpha particles in an ionization chamber. These circuits sort the pulses according to size and record them on 48 separate registers.

3. Gamma Analyzer.

Gamma rays were analyzed by a 50-channel gamma-ray pulse analyzer in which the detecting unit is a sodium iodide (thallium activated) scintillation crystal. Counting efficiency varies with gamma-ray energy.[35]

4. Geiger-Müller Counter.

The beta particles emitted by the fission products were counted with a Geiger-Müller counter in which the counting unit was an end-window Amperex 100 C tube filled with a mixture of chlorine and argon. The tube and sample were housed in a thick-walled lead case to reduce background effects. Samples could be placed in any of five fixed positions ranging from 0.46 to 6.81 cm from the window of the tube. When activity of the sample permitted, the samples were placed on Shelf 2, which is 2 cm from the window. The geometry of Shelf 2 with respect to the detecting unit for the particular counter used was determined to be 3.25 percent. The counter was operated on the G-M plateau, which was found to have a slope of approximately 10 percent per 100 v. The dead-time value is 0.45 percent per 1000 counts.[36]

5. Nucleometer.

The Nucleometer contains a methane flow-type windowless proportional

counter. The high efficiency of this counter made it particularly favorable for following the decay of low-intensity beta-particle emitters. The plateau was determined for each isotope and the samples were always counted at this voltage range. The counting efficiency increases with increasing beta-particle energy.

III. TREATMENT OF DATA

A. Yield Determination

For each actinide element isolated, a known amount of an alpha-emitting isotope was added to the target solution. Yield was determined from the amount of that particular isotope remaining in the isolated fraction. For fission products, a known amount of inactive carrier was added for each product isolated and the yield was determined by weighing the separated fission product.

B. Isotope Identification

Energy and half-life data were used to identify isotopes. The only alpha activity produced in measurable amount in the bombardment series was that of Pu^{238}. It was identified by its 5.5-Mev alpha particles. Usually the beta-particle emitters were identified by their half-lives, which were resolved from decay curves. This could not be done for Np^{238} ($t_{1/2}$ = 2.1 days) and Np^{239} ($t_{1/2}$ = 2.33 days). These isotopes were distinguished by gamma analysis.

C. Decay Curve Resolution

Approximately five counts were taken during each half-life period of the shortest-lived isotope in each sample. The counts per minute were corrected for counter dead time and background, and plotted versus the time elapsed from the end of the bombardment. In cases where several activities were contained in one sample, the curve was resolved by subtracting out the activities. The activity of a particular isotope at the end of the bombardment was determined analytically from its activity at any given time by use of the formula:

$$A = A_o \exp - \frac{0.693t}{t_{1/2}}$$

where A = activity at time t,

A_o = activity at end of bombardment

$t_{1/2}$ = half-life of the isotope

D. Calculation of Disintegrations per Minute

Alpha ionization chamber counts per minute were converted to disintegrations per minute by dividing the counts per minute by the geometry factor, 0.52.

Similarly, the number of disintegrations per minute of Nucleometer-counted isotopes was determined by dividing the counts per min of each isotope by its counting efficiency. The counting efficiency of beta particles in the Nucleometer depends on both the percent of beta particles counted directly and the percent of backscattered particles that are counted. Because the 2π chamber of the Nucleometer was used, 50 percent of the beta particles were counted directly. With platinum backing material, approximately 20 percent to 80 percent of the backscattered beta particles are counted, depending on the energy of the beta particles. The counting efficiency values used in calculating disintegrations per min of all isotopes counted on the Nucleometer in this bombardment series are listed in Table I. Since it is difficult to determine beta counting efficiencies, the values listed may be in error by as much as 15 percent. Thus the counting efficiency values used are to be regarded as preliminary estimates, subject to revision when better absolute beta particle counting data become available.

TABLE I

Estimated Counting Efficiency Factors

Isotope	Beta Particle Energy	Counting Efficiency
U^{237}	0.25, 0.08	0.66
Np^{238}	1.26, 0.26	0.80
Np^{239}	0.33, 0.44	0.70
Np^{240}	2.16, 1.59, 1.26	0.85

Counts per min observed on the Geiger-Müller counter were converted to disintegrations per min by use of the formula:

$$d/m = c/m \times \frac{A.W. \times Ceff}{BS \times SSSA \times g}$$

where the correction factors are as set forth below.

1. A. W.- Air and Window Absorption and Scattering Factor.

Some of the beta particles are absorbed and scattered by the 5.9 mg/cm^2 (3.5 $\frac{mg}{cm^2}$ mica window plus 2.4 mg/cm^2 of air) between Shelf 2 and the window of the tube. Since for light elements, the absorption thickness is nearly independent of the nature of the absorber,[37] this correction factor was evaluated for beta particles of various energies by extrapolating the initial portion of aluminum absorption curves. This was not possible when the sample emitted two or more beta groups similar in energy. In this case, the A. W. correction was evaluated from a curve of experimentally determined A. W. correction versus beta energy.

2. Ceff-Counting Efficiency Correction.

It was assumed that all beta particles getting through the mica window of the counter would count. (Therefore Ceff = 1.0)

3. B. S. - Backscattering Correction.

Correction factors determined by Burtt[38] for the beta particles backscattered by the aluminum sample support were used.

4. SSSA - Self-Scattering and Self-Absorption Correction.

The self-scattering and self-absorption effects of certain fission products have been determined by Hicks, Stevenson, and Gilbert.[39] Correction factors were taken from their curves whenever applicable. When this was not possible, the correction factors were estimated from the data of Stevenson and Nervik.[40] The latter workers determined the variation of the SSSA factor with beta-particle energy and thickness of sample, using homogeneous mixtures of carrier-free beta-particle emitters and inactive salts. Since SSSA corrections vary with atomic numbers of both anion and cation of the sample, the correction factor for each fission product isotope was determined by interpolating the data from their sodium chloride and lead nitrate curves on the basis of the summed atomic numbers of the atoms in the molecule. This factor was evaluated for each fission product isotope in every bombardment.

5. g - Geometry Correction.

The geometry factor represents the fraction of the total number of beta particles emitted by the source that actually reaches the detector. This factor was determined by using known standards. This factor was found to be 3.25 percent for Shelf 2.

The backscattering and air-window correction factors used in calculating the disintegrations per min of each fission product isotope observed are listed in Table II.

TABLE II

Backscattering and Air-Window Correction Factors [a]

Isotope	$t_{1/2}$	β^- Energy (Mev)	A. W.	B. S. [b]
Ag^{111}	7.6 d	1.04 (91%); 0.70 (8%)	1.14	1.28
Ag^{113}	5.3 h	2.0	1.02	1.28
Ba^{139}	85 m	2.27	1.02	1.28
Ba^{140}	12.8 d	1.022 (75%); 0.48 (25%)	1.21	1.28
Cd^{115m}	43 d	1.61	1.05[c]	1.28
Cd^{115}	54 h	0.58 (42%); 1.1 (58%)	1.10[c]	1.27
Cd^{117}	2.9 h	1.6; 3.0	1.02	1.28
Ce^{141}	33 d	0.58 (33%); 0.44 (67%)	1.48[c]	1.24
Ce^{143}	33 h	1.4 (30%); 1.1 (40%); 0.7 (30%)	1.15	1.28
Eu^{156}	15.4 d	0.5 (60%); 2.4 (40%)	1.31[c]	1.26
Eu^{157}	15.4 h	1.0 (75%); 1.7 (25%)	1.11[c]	1.28
Gd^{159}	18.0 h	0.90	1.19	1.28
In^{115m}	4.5 h	0.83	1.23	1.28
In^{117m}	2.5 h	1.7	1.03	1.28
Mo^{99}	67 h	1.23 (80%); 0.45 (20%)	1.14[c]	1.28
Nb^{95}	35 d	0.16	1.9	1.08
Nb^{97}	72 m	1.3	1.06	1.28
Nd^{147}	11.6 d	0.83 (60%); 0.60 (15%); 0.38 (25%)	1.25[c]	1.26
Pd^{112}	21 h	0.20	1.78[c]	1.13
Ru^{103}	40 d	0.22 (65%); 0.2 (35%)	2.25	1.12
Ru^{105}	4.5 h	1.15	1.09[c]	1.28

TABLE II (Cont'd)

Isotope	$t_{1/2}$	β^- Energy (Mev)	A. W.	B. S.[b]
Rh^{105}	36.5 h	0.57	1.35	1.26
Sr^{89}	50.4 d	1.46	1.04[c]	1.28
Sr^{91}	9.7 h	2.65 to 1.09	1.07	1.28
Te^{127}	9.3 h	0.70	1.32[c]	1.26
Te^{129}	70 m	1.8	1.04	1.28
Te^{132}	77.7 h	0.22	1.73	1.13
Tb^{161}	70 d	0.50	1.43	1.25
Y^{91}	61 d	1.5	1.04	1.28
Zr^{95}	65 d	0.37	1.53[c]	1.26
Zr^{97}	17 h	1.9	1.04[c]	1.28

a. These corrections apply only to Geiger-Müller counters having the same air-window thickness, (5.9 mg/cm^2).

b. B. S. corrections are taken from Burtt's curves.[38]

c. These air-window corrections have been experimentally determined. The others have been estimated.

E. Corrections for Conversion Electrons

An appreciable amount of the radiation detected by the Geiger-Müller counted from Ru^{105} and Cd^{115} samples was due to conversion electrons from their daughters. Because of the lack of data on backscattering and self-scattering corrections of conversion electrons, the approximation made was that a conversion electron would have the same BS and SSSA correction factor as a beta particle with three times as much energy as the conversion electrons. No air-window correction was made for conversion electrons because they are monoenergetic.

F. Parent-Daughter Relationships

Corrections for a daughter beta activity were made by use of the formula:

$$N_2 = \frac{\lambda_1}{\lambda_2 - \lambda_1} N_1^0 (e^{-\lambda_1 t} - e^{-\lambda_2 t}),$$

where N_2 is the number of atoms of the daughter present at time t, N_1^0 is the number of atoms of parent nuclide at the end of the bombardment, and λ_1, and λ_2 are decay constants of the parent and daughter respectively.

G. Cross-Section Calculations

The number of atoms of the fission and spallation products produced in the bombardment was calculated by means of the formula:

$$N = d/m \quad \frac{t_{1/2}}{0.693 \text{ (chemical yield)}},$$

where d/m is the number of disintegrations per min at the end of bombardment and $t_{1/2}$ is the half-life of the isotope, cross-sections were then calculated from the formula:

$$\sigma = \frac{N}{n/cm^2} (It),$$

where N is the number of atoms produced, n/cm^2 is the density of the U^{238} target atoms and It is the total number of alpha particles striking the target. When the half-life of the isotope was short and appreciable decay took place during the bombardment, the formula used was:

$$\sigma = \frac{0.693 \text{ N}}{t_{1/2} (n/cm^2) (I) (1-e^{-\lambda t})},$$

where N is the number of atoms at the end of bombardment, I is the beam intensity, $t_{1/2}$ is the half-life of the isotope, λ is the decay constant of the isotope, and t is the length of time the target was bombarded. This formula can be used only when I is constant. In these bombardments I was essentially constant. The target and beam factors used in calculating cross-sections are listed in Table III.

Table III

Target and beam factors				
Energy (Mev)[a]	mg U^{238}	target area (cm^2)	n/cm^2	It
22.6	0.560	1.08	1.32×10^{18}	9.55×10^{16}
25.2	0.713	1.00	1.81×10^{18}	1.2×10^{17}
27.1	0.670	1.02	1.67×10^{18}	1.33×10^{17}
32.5	0.435	0.88	1.35×10^{18}	1.53×10^{17}
33.8	0.202	0.95	5.4×10^{17}	1.18×10^{17}
37.9	0.498	0.95	1.33×10^{18}	1.32×10^{16}
38.6	0.257	0.82	7.9×10^{17}	2.72×10^{16}
38.6	0.795	0.95	2.1×10^{18}	1.33×10^{17}
40[b]	1-mil foil		0.49×10^{20}	9×10^{17}
41.4	0.435	0.88	1.25	1.36×10^{17}
43.9	0.382	0.96	1.01×10^{18}	8.15×10^{16}
45.9	0.512	0.88	1.47×10^{18}	8.52×10^{16}

a. The energy uncertainty is estimated to be ± 0.5 Mev.

b. The energy in this foil bombardment ranged from about 38 to about 42 Mev.

IV. RESULTS

A. Spallation Cross Sections

The spallation cross sections of U^{238} are listed in Table IV. Energy thresholds are listed below the products. These thresholds were calculated from the formula:

$$\text{Threshold (Ea)} = Q \frac{M\ Pu^{242}}{M\ Pu^{238}} = Q \frac{242}{238},$$

where I = nuclear reaction energy. Figure 2 shows the spallation excitation functions.

Experiments by Michel and Lessler[28] indicate that the 60-min neptunium activity, which had been previously identified as Np^{241}, is actually an isomer of Np^{240}. Therefore, the cross section for this 60-min activity is reported as an (α, pn) rather than an (α, p) reaction.

No evidence of the 15-min Np^{241} activity reported by Lessler[28] was observed. In two bombardments especially designed to permit observation of this activity, the neptunium fraction was isolated within one hour of the end of bombardment. These two experiments indicate that the upper limit of the formation cross section of this 15 min activity is 0.01 mb at 37 Mev.

B. Fission Product Cross Sections

Fission product cross sections are listed in Table V. The curves of fission product yield versus mass are presented in Fig. 3-9. The error in determining the absolute fission yield is estimated to be about 20 percent. Total fission cross sections and spallation cross sections are compared in Fig. 10. The assumption was made that the fission product cross sections reported represent the total yield of the mass chain. There are indications that this assumption may not be valid at the higher energies.[41] The shape of the fission-yield curves was determined from both experimental and reflected points.

Table IV

U^{238} + α Spallation cross sections (millibarns)

Product	Pu^{238}	Np^{240} (60 min)	Np^{239}	Np^{238}	U^{237}
Reaction	α, 4n	α, pn	α, p2n	α, p3n	α, αn
Threshold (Mev)	29.2	18.3	23.4	29.6	6.52
Energy (Mev)					
22.6		0.027 ± 0.007	0.29 ± 0.04		
25.2		1.2 ± 0.18	1.4 ± 0.21		0.55 ± 0.14
27.1		1.3 ± 0.20	12.0 ± 1.8		3.0 ± 0.75
32.5		1.9 ± 0.29	11.8 ± 1.8		9.9 ± 2.5
33.8	9.1 ± 1.8	4.0 ± 0.60	12.2 ± 1.8		16.0 ± 4.1
37.9		6.6 ± 0.90			
38.6	17.0 (on green)	6.8 ± 1.0	23.0 ± 3.5		100 ± 25
			27.0 ± 4.1		91.0 ± 23
40.0				3.8 ± 0.95	
41.4	69 ± 14	7.0 ± 1.1	28.0 ± 4.2		
43.9	44 ± 8.8				110 ± 28
45.4	9.6 ± 1.9	5.9 ± 0.9	44.0 ± 6.6	8.8 ± 2.2	150 ± 38

Table V

Fission products cross sections[a] (millibarns)

Isotope	Alpha Energy								
	22.6	25.2	27.1	32.5	33.8	38.6	40.1	43.9	45.4
Sr^{89}							24		27
Sr^{91}							27		35
Zr^{95}	4.7		29	21	28	38	35	41	36
Zr^{97}	8.0		36	34	41	54	54	53	52
Mo^{99}							59		
Ru^{103}	6.5					47	44	51	47
Ru^{105}	7.0					36	53	55	48
Pd^{112}							54		
Ag^{111}							43[b]		
Ag^{113}							49		
Cd^{115}	2.6		15.4			48	60	58	49
Cd^{117}	1.9[c]							61[c]	
Te^{129m}							31[b]		
Te^{132}							39[c]		
Ba^{139}	6.5					36		37	42
Ba^{140}	5.8				29	35	35	36	36
Ce^{141}			40						
Ce^{143}		11.5	23			44	49	30	

Table V (cont.)

Fission products cross sections[a] (millibarns)									
Isotope	Alpha Energy								
	22.6	25.2	27.1	32.5	33.8	38.6	40.1	43.9	45.4
Nd^{147}			15			27	19		
Eu^{156}			1.8			3.4	4.1		
Eu^{157}			1.5			2.5	2.2		
Gd^{159}							0.71		
Jb^{161}			0.29			0.46			
Total fission cross section	150		770			1,390	1,600	1,540	1,500
Number of neutrons out	2		4			6	6	6	8

a. Probable error is about 20%.

b. Cross section is for one isomer only.

c. Cross section is approximate owing to complexities in the decay scheme.

V. DISCUSSION

The reactions of U^{238} with low-energy helium ions can be represented by the following isotope diagram.

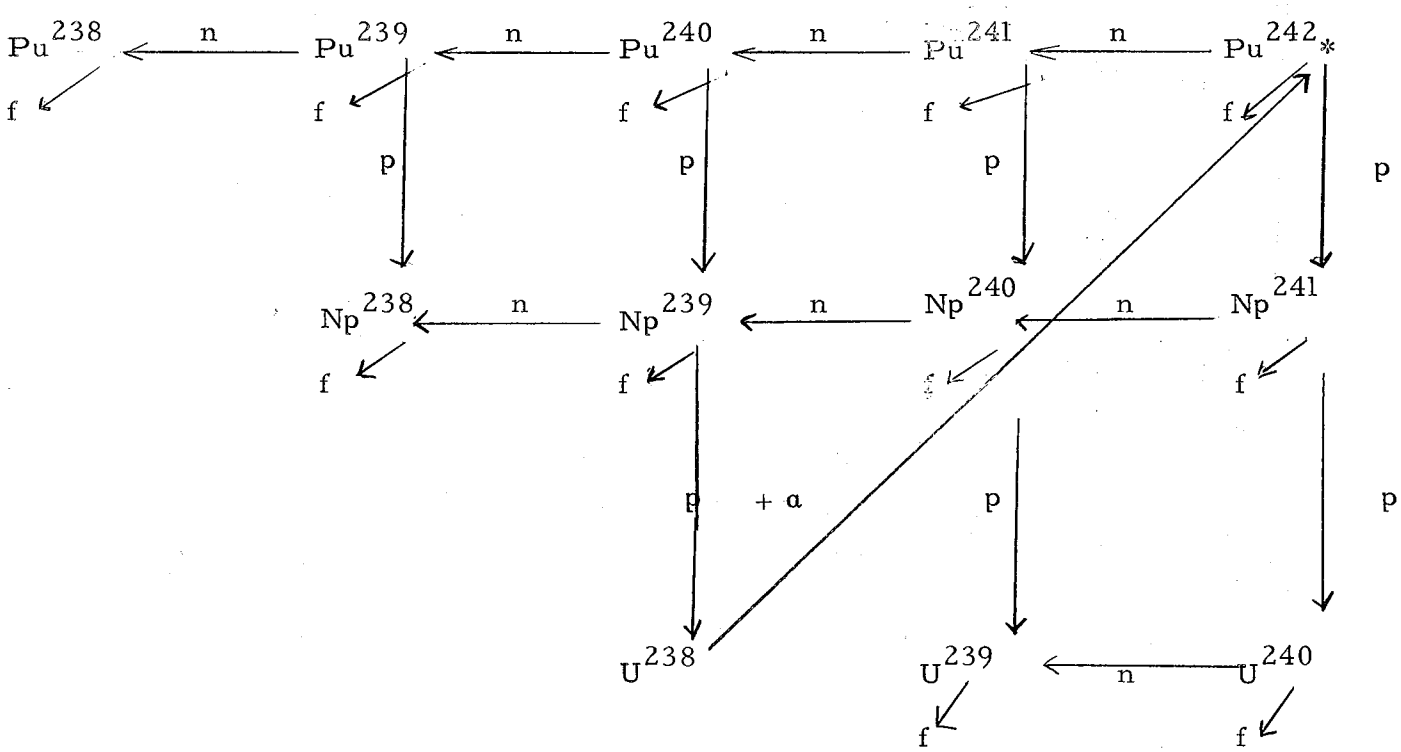

In this type of representation, it is assumed that the U^{238} nucleus captures an alpha particle to form the excited compound nucleus $Pu^{242}*$. The arrows refer to the paths along which the compound nucleus can de-excite by a stepwise process. Thus $Pu^{242}*$ can de-excite by neutron emission, proton emission, or fission. If the product nuclide resulting from neutron or proton emission of Pu^{242} has sufficient excitation energy, it can also de-excite be neutron emission, fission, or possibly proton emission. Complete de-excitation by gamma-ray emission becomes competitive after one particle has "boiled out". With increasing energy of the bombarding helium ion, the excitation energy of the compound nucleus is increased, and therefore, reaction products formed by ejection of several particles from the compound nucleus become more prominent. The excitation energy of the compound nucleus is given by the formula:

$$E_{ex} = E_{\alpha} \frac{238}{242} - 5.0 ,$$

where E_α is the energy of the bombarding helium ions and 5.0 is the mass energy required for compound nucleus formation.

A. Spallation Reactions

The activities due to (α, n), (α, 2n), and (α, 3n) products were insufficient for detection by standard counting techniques. Therefore, cross-sections for these reactions could not be determined. Since these reactions have been found to be prominent[10, 42, 43] in bombardments of other nuclides with atomic numbers greater than 81, the total yield of spallation products produced in bombardment of U^{238} with helium ions could not be determined. For this reason, the total spallation yield of U^{238} cannot be compared with that of nuclides of different atomic number. However, comparison of specific spallation reactions of U^{238} with the same spallation reactions of nuclides of different atomic number confirms the observed trend of decreasing spallation yield with increasing atomic number of the target nuclide in the heavy-element region.

A surprising result is the sharp rise and fall w th energy of the (α, 4n) cross-section, which peaks at 41 Mev. The (α, 4n) cross-sections of Pu^{239}, Cm^{244},[43] and Pb^{208},[44] are still rising at this energy. Glass[10] found that the magnitude of the (α, xn) cross-sections decreased with increasing x (for values of x greater than 1). On this basis, the peak values of the cross-sections of the (α, 2n) and (α, 3n) reactions of U^{238} are probably greater than 64 mb, which is the peak value of the U^{238} (α, 4n) Pu^{238} cross-section.

The (α, pn) cross-section may be higher than the value reported, since only the 60-min isomer was observed. In contrast with the (α, xn) reactions, the magnitude of the (α, pn) reaction seems to vary little with mass and atomic number of the target nuclide in the heavy-element region. Approximate values of the (α, pn) cross-sections of various nuclides at about 40 Mev are:

Pb^{208}	8 mb[45]
U^{233}	7 mb[46]
Pu^{238}	4 mb[42]
U^{238}	7 mb

There are two reasons for thinking that the (α, pn) absolute cross-sections should show a marked decrease with increasing Z. First, according to compound-

nucleus theory, proton emission becomes less probable with increasing Z because of the coulomb barrier. Second, the chance of the (α, pn) products being destroyed by fission increases with increasing Z. To this extent, the magnitude of the (α, pn) cross-sections does not agree with predictions of the compound-nucleus theory. Although the absolute magnitude of the (α, pn) cross-section remains nearly constant with Z, the ratio of the (α, pn) to the (α, xn) reactions increases with Z. This indicates that the probability that fission will destroy the (α, xn) products increases more rapidly with Z than the probability that fission will destroy the (α, pn) products.

A high(α, p2n) cross-section seems to be characteristic in the heavy-element region.[10, 42, 46, 47] Of particular interest is the fact that the U^{238} (α, p2n) Np^{239} reaction is observed at 22.6 Mev. The threshold for evaporation of two neutrons and a proton from the compound nucleus, Pu^{242}, is 23.4 Mev. The threshold for tritium emission, however, is 14.4 Mev. Since threshold requirements are strict, it seems likely that the (α, p2n) product is formed by tritium emission when the energy of the bombarding helium ion is less than 23.4 Mev. At higher energies, the (α, p2n) product may be formed by both paths. Experiments designed to permit detection of tritium are now in progress in this laboratory.[48]

The (α, p3n) cross-section begins to rise after the (α, 4n) cross-section has reached its peak. This is in accord with compound-nucleus theory, since greater excitation energy is required to overcome the coulomb barrier in proton emission.

Some attempts were made to detect the (α, 2p) and (α, 2pn) reactions. In the bombardment at 45.4 Mev, some 14-hr activity, which may be due to the (α, 2p) product, U^{240}, was observed. The value obtained for this cross-section was 6 mb. However, the uranium sample contained some impurity, and therefore, the results were considered to be inconclusive. Further investigations of these reactions are planned.

The (α, αn) reaction was the most prominent spallation reaction observed in this series. It is doubtful that compound-nucleus formation is taking place in this reaction, since the coulomb barrier tends to prevent alpha-particle emission. A possible mechanism for this reaction is a direct interaction of the bombarding particle with the diffuse rim of the nucleus, resulting in local excitation and subsequent emission of a nucleon. In this case, the (α, αp) cross-section should also be prominent because of the increased chance (over

compound-nucleus formation) that a proton will have a high excitation energy. Another possibility is a process in which the scattered helium ion transfers some of its kinetic energy to the entire target nucleus. After many energy interchanges, a sufficient amount of energy concentrates on one nucleon so that it can escape. With this second type of mechanism, the (α, αp) reaction should be much smaller than the (α, αn) reaction, because the proton has a relatively smaller chance of having sufficient energy to penetrate the coulomb barrier.

B. Fission Yields

The expected increase in symmetry of fission with energy was observed. The broad flat peak of the curve for fission yield versus mass at 40 Mev indicates that both symmetric and asymmetric fission are occurring at this energy. The minimum in this curve disappears at approximately the same energy as in helium ion bombardments[10] of Pu^{239}. However, data given by Gilbert and Hicks[49] indicate that in deuteron and proton bombardments of U^{238}, this minimum does not disappear until energies of 50 to 100 Mev for deuterons and 170 to 250 Mev for protons are reached. Also, Jungerman and Wright[50] observed evidence of asymmetric fission when bombarding U^{238} with 45-Mev neutrons. Since deuterons, protons, and neutrons give only 5 to 10 Mev higher excitation energy to the compound nucleus than helium ions of the same energy, there seems to be a discrepancy. Different types of compound nuclei are formed with these various bombarding particles, and therefore the effect may be due to a variation of fission symmetry with nuclear type.

In order to obtain reflection points for the curves, it was necessary to make an assumption regarding the number of neutrons emitted per fission, where one number admittedly does not apply for the entire yield curve. At each energy that value was chosen which gave the smoothest fission-yield curve. This varied from two neutrons at 22.6 Mev to eight neutrons at 45.4 Mev. This same trend was observed with helium-ion-induced fission[51] of Pu^{239}. Although fission-yield curves indicate the number of neutrons given off, they give no information as to whether the neutrons are given off before or after fission. If fission occurred before neutron evaporation, the energy of the fission fragments should increase with increasing energy of the bombarding particle, since the excitation energy of the compound nucleus is higher. Douthett and Templeton's experiments show that the range of fission fragments produced in high-energy projectile-induced fission is the same as the range of those produced in low-energy fission. Thus prefission evaporation of the two to eight neutrons from U^{238} nucleons

seems most likely.

Fission was found to be the most prominent reaction for all bombarding energies in this series. The total fission cross-section, determined by integrating the fission-yield curves, rises rapidly at the lower energies, and levels off at a value of 1.5 barns at 38 Mev. This agrees with the value of 1.4 barns taken from Jungerman's[53] graph for total fission cross-section of U^{238} bombarded with 38-Mev helium ions. The method of counting fission pulses with an ionization chamber was used. Newton[7] found the total fission cross-section of Th^{232} bombarded with 37.5-Mev helium ions to be 0.6 barns. The higher fission cross-section of U^{238} can be attributed to increased fissionability with increasing Z^2/A. Although the fission cross-section[51] of Pu^{239} at 37 Mev is only 0.5 barns, this does not necessarily indicate a discrepancy, since the total fission cross-section of Pu^{239} is still rising at 48 Mev. This may be a reflection of the increased stability of odd-nucleon nuclides toward fission.

In Fig. 11, the total fission excitation function is compared with a theoretical reaction cross-section curve. The fission cross-section alone is higher than the highest theoretical total reaction cross-section and, since undetermined spallation cross-sections undoubtedly are appreciable, the experimental total reaction cross-section must be still higher. This implies either a large nuclear radius (larger than calculated by an r_0 value of 1.5×10^{-13}) or that the theoretical treatment is inadequate. The total reaction cross-section is probably a large fraction of the 2.8-barn geometric cross-section (calculated on the basis of $r_0 = 1.5 \times 10^{-13}$) above 40 Mev.

ACKNOWLEDGMENTS

I wish to thank Professor Glenn T. Seaborg for his interest and guidance. I wish to thank Richard A. Glass, Bruce M. Foreman, Walter M. Gibson, E. Victor Luoma, T. Darrah Thomas, Robert Vandenbosch and William Wade for their helpful discussions and experimental aid. The discussions with Earl K. Hyde are also appreciated, as is the assistance of Therese K. Pionteki in counting the samples. The cooperation of Professor Joseph G. Hamilton, G. Bernard Rossi, W. Bart Jones, and the crew of the 60-inch cyclotron is gratefully acknowledged. The aid of the Health Chemistry Group and particularly that of Sue Hargis and Roberta Delk is appreciated.

This work was performed under the auspices of the U.S. Atomic Energy Commission.

REFERENCES

1. R. W. Spence and G. P. Ford, Annual Reviews of Nuclear Science (Stanford University Press, Stanford, Calif., 1953), 2, 399.
2. N. Bohr and J. A. Wheeler, Phys. Rev. 56, 425 (1939).
3. E. P. Steinberg and M. S. Freedman, Radiochemical Studies: The Fission Products (McGraw-Hill Book Company, Inc., New York, 1951) National Nuclear Energy Series, Plutonium Project Record, 9, p. 1378.
4. P. Kruger and N. Sugarman, Phys. Rev. 99, 1959 (1955).
5. R. H. Goeckermann and I. Perlman, ibid., 82, 628 (1949).
6. Folger, Stevenson, and Seaborg, ibid., 98, 107 (1955).
7. A. S. Newton, ibid., 75, 17 (1949).
8. H. A. Tewes and R. A. James, ibid., 88, 860 (1952).
9. Fowler, Jones, and Paehler, ibid., 88, 7 (1952).
10. R. A. Glass, Ph.D. Thesis, University of California Radiation Laboratory Unclassified Report UCRL-2560 (April 1954).
11. A. Turkevich and J. B. Niday, Phys. Rev. 84, 52 (1951).
12. J. M. Blatt and V. F. Weisskopf, Theoretical Nuclear Physics (John Wiley and Sons, Inc., New York, 1952), p. 340.
13. S. N. Ghoshal, Phys. Rev. 80, 939 (1950).
14. B. L. Cohen, ibid., 98, 25 (1955).
15. E. R. Graves and L. Rosen, ibid., 89, 1343 (1953).
16. P. C. Gugelot, ibid., 81, 51 (1951).
17. B. L. Cohen, ibid., 92, 1245 (1953).
18. E. B. Paul and R. L. Clarke, Can. J. Phys. 31, 267 (1953).
19. Cohen, Newman, Charpie, and Handley, Phys. Rev. 94, 620 (1954).
20. Cohen, Newman, and Handley, ibid., 99, 723 (1955).
21. J. Konopinski and H. A. Bethe, ibid., 54, 130 (1938).
22. H. McManus and W. T. Sharpe, ibid., 87, 188 (1952).
23. R. Serber, ibid., 72, 1114 (1947).
24. Aron, Hoffman, and Williams, U.S. Atomic Energy Commission Unclassified Document AECU-663 (May 1951).
25. D. L. Hufford and B. F. Scott, The Transuranium Elements: Research Papers (McGraw-Hill Book Company, Inc., New York, 1949), National Nuclear Energy Series, Plutonium Project Record, Vol. 14B, p. 1149.
26. A. F. Kovarik and N. I. Adams, Jr., Phys. Rev. 98, 46 (1955).

27. T. D. Thomas, unpublished data (1955).
28. R. M. Lessler, University of California Radiation Laboratory Unclassified Report UCRL-2647 (July 1954).
29. Magnusson, Huizenga, Siddall, and Studier, Argonne National Laboratory Classified Report ANL-4667 (May 1951).
30. W. W. Meinke, University of California Radiation Laboratory Unclassified Report UCRL-432 (August 1949).
31. C. D. Coryell and N. Sugarman, Radiochemical Studies: The Fission Products (McGraw-Hill Book Company, Inc., New York, 1951), National Nuclear Energy Series, Plutonium Project Record, Vol. 9.
32. M. Lindner, University of California Radiation Laboratory Unclassified Report UCRL-4377 (August 1954).
33. W. E. Nervik, J. Phys. Chem. 59, 690 (1955).
34. Ghiorso, Jaffey, Robinson, and Weissbound, The Transuranium Elements: Research Papers (McGraw-Hill Book Company, Inc., New York, 1949), National Nuclear Energy Series, Plutonium Project Record, Vol. 14B, p. 1226.
35. M. I. Kalkstein and J. M. Hollander, University of California Radiation Laboratory Unclassified Report UCRL-2764 (October, 1954).
36. H. P. Robinson, unpublished data.
37. S. Glasstone, Sourcebook on Atomic Energy (D. Van Nostrand Company, New York, 1950) p. 65.
38. B. P. Burtt, Nucleonics, 8, 28 (1949).
39. Hicks, Stevenson, and Gilbert, unpublished data (1953).
40. W. E. Nervik and P. C. Stevenson, Nucleonics 10, 18 (1952).
41. W. M. Gibson, unpublished data (1955).
42. R. J. Carr, Ph.D. Thesis, University of California (December 1955).
43. A. Chetham-Strode, Ph.D. Thesis, University of California (1956).
44. W. John, University of California Radiation Laboratory Unclassified Report UCRL-3093 (August 1955).
45. Templeton, Howland, and Perlman, Phys. Rev. 72, 758 (1947).
46. T. D. Thomas, unpublished data (1955).
47. R. Vandenbosch, unpublished data (1955).
48. W. Wade, private communication.
49. H. G. Hicks and R. S. Gilbert, University of California Radiation Laboratory Unclassified Report UCRL-4506 (May 1955).

50. J. Jungerman and S. C. Wright, Phys. Rev. 76, 1112 (1949).

51. Glass, Carr, Cobble, and Seaborg, to be published.

52. E. M. Douthett and D. H. Templeton, Phys. Rev., 94, 128 (1954).

53. J. Jungerman, ibid., 79, 632 (1950).

54. R. A. Glass, extrapolated from values given in tables by J. M. Blatt and V. F. Weisskopf, Theoretical Nuclear Physics (John Wiley and Sons, New York, 1952), p. 353.

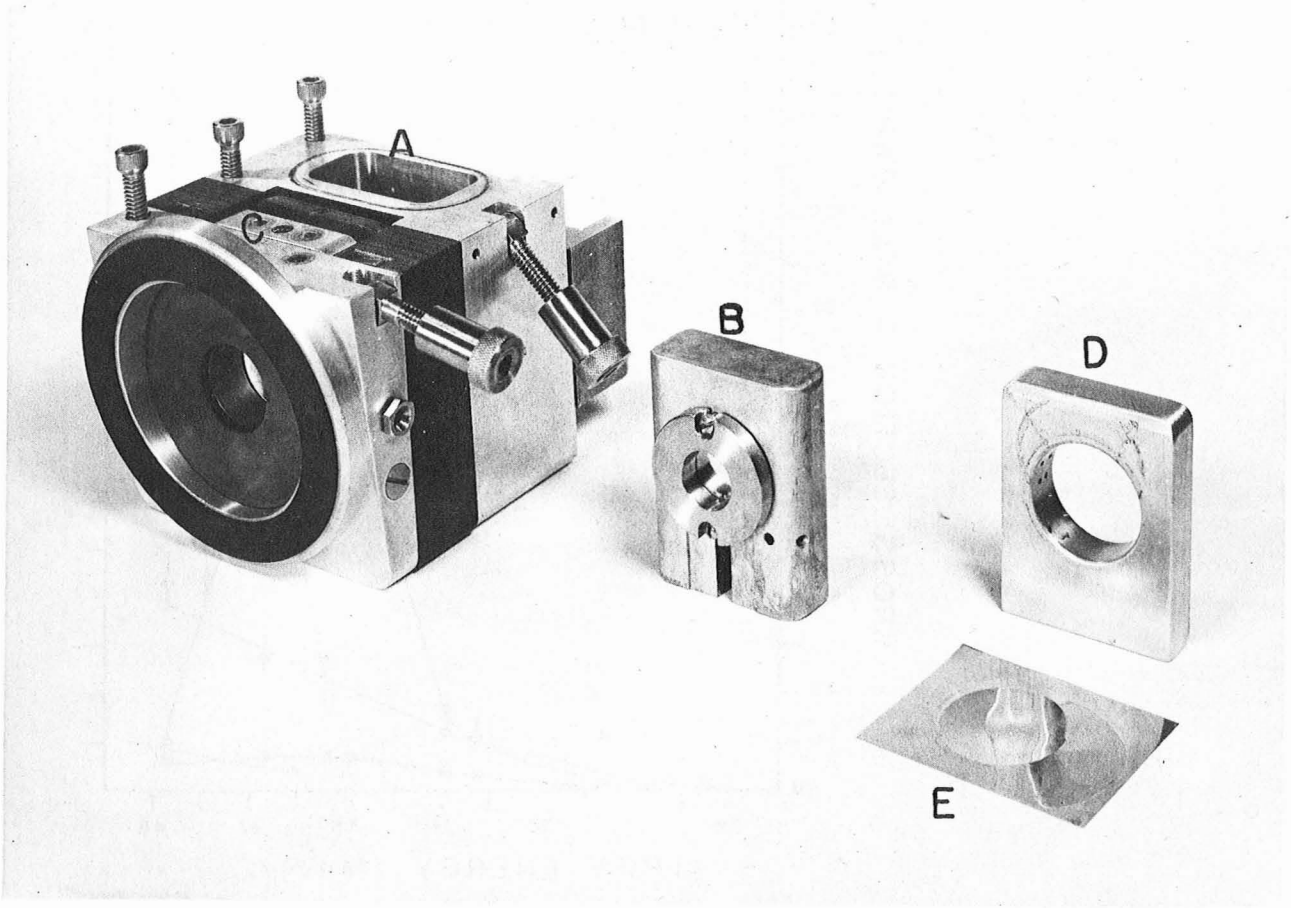

ZN-1412

Fig. 1. Microtarget assembly. A Microtarget slot, B Microtarget, C Collimator, D Foil holder, E Degrading foil.

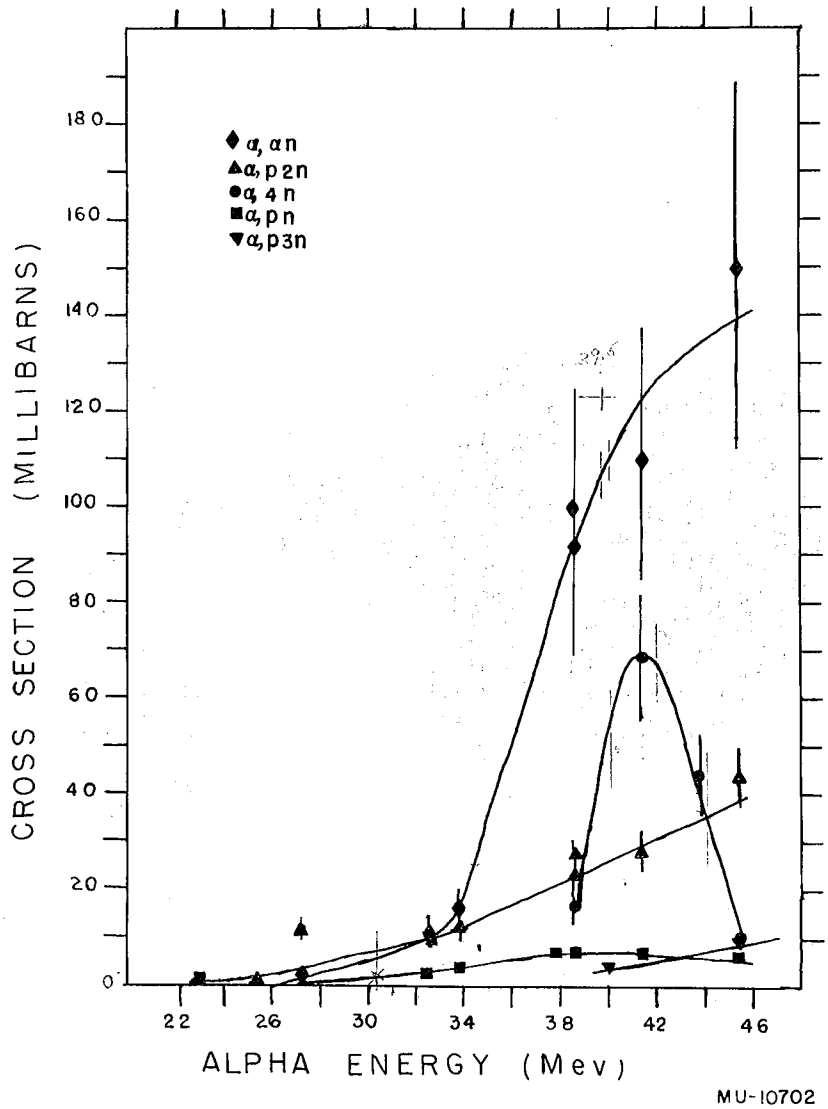

Fig. 2. Excitation curves for some spallation products formed in bombardments of U^{238} with helium ions in the energy range of 22 to 46 Mev.

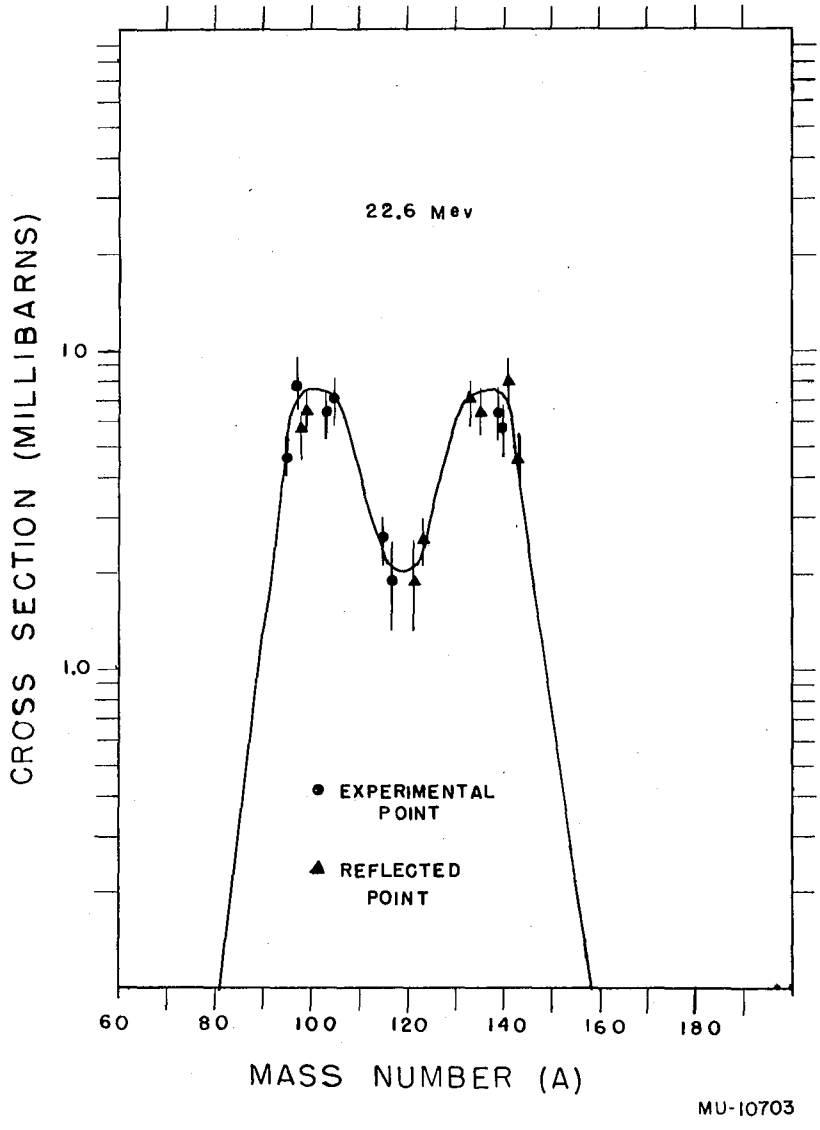

Fig. 3. Fission yield versus mass curve of the fission products formed in bombardment of U^{238} with 22.6 Mev helium ions.

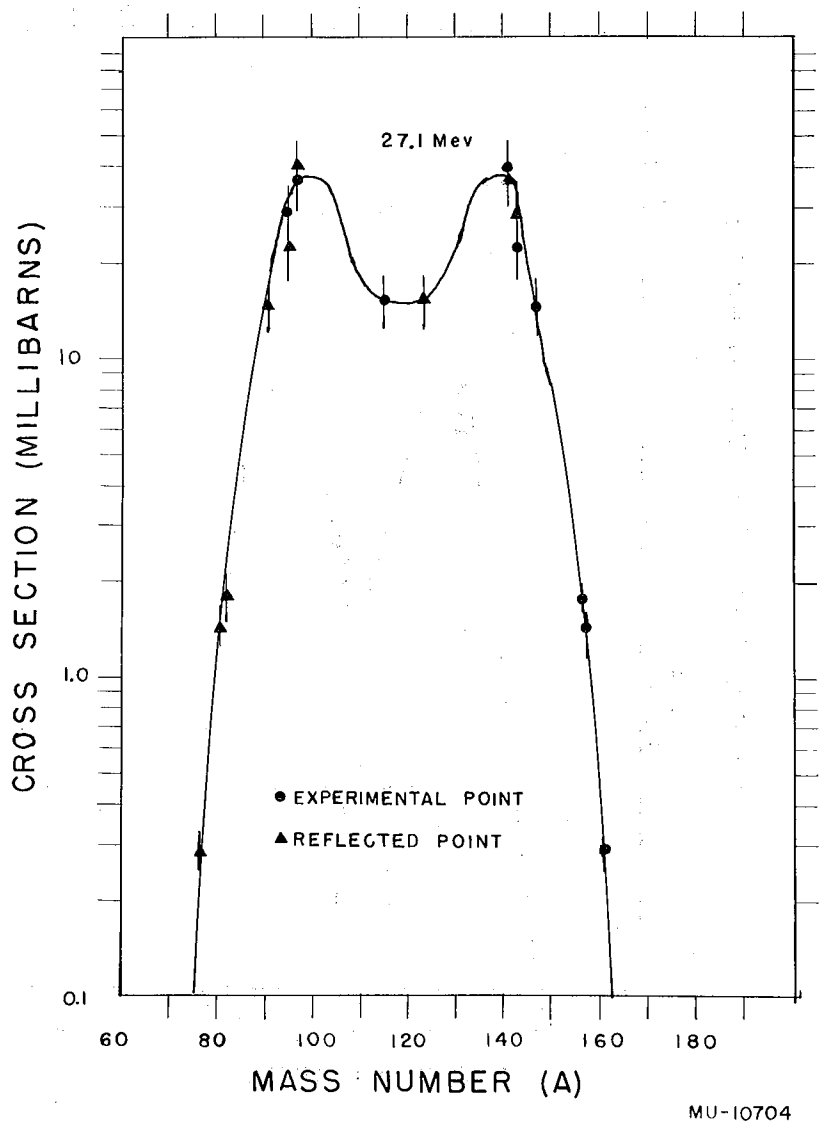

Fig. 4. Fission yield versus mass curve of the fission products formed in bombardment of U^{238} with 27.1 Mev helium ions.

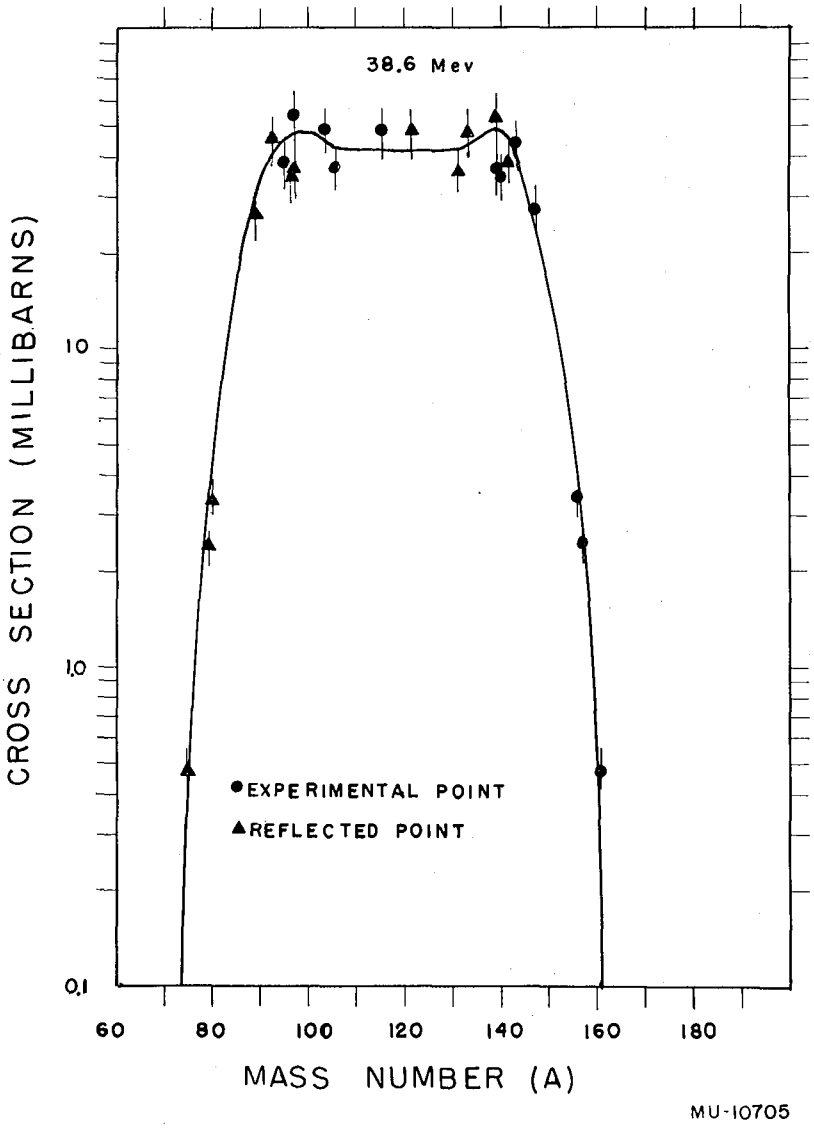

Fig. 5. Fission yield versus mass curve of the fission products formed in bombardment of U^{238} with 38.6 Mev helium ions.

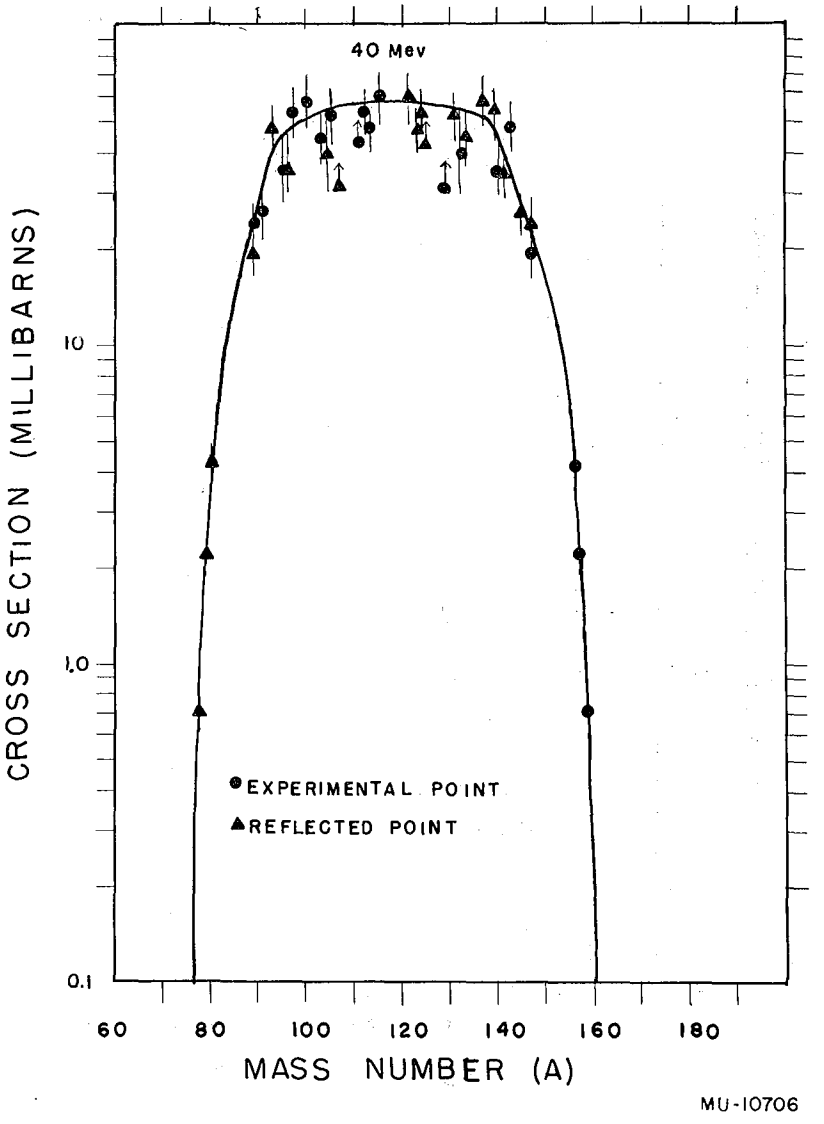

Fig. 6. Fission yield versus mass curve of the fission products formed in bombardment of U^{238} with 40 Mev helium ions.

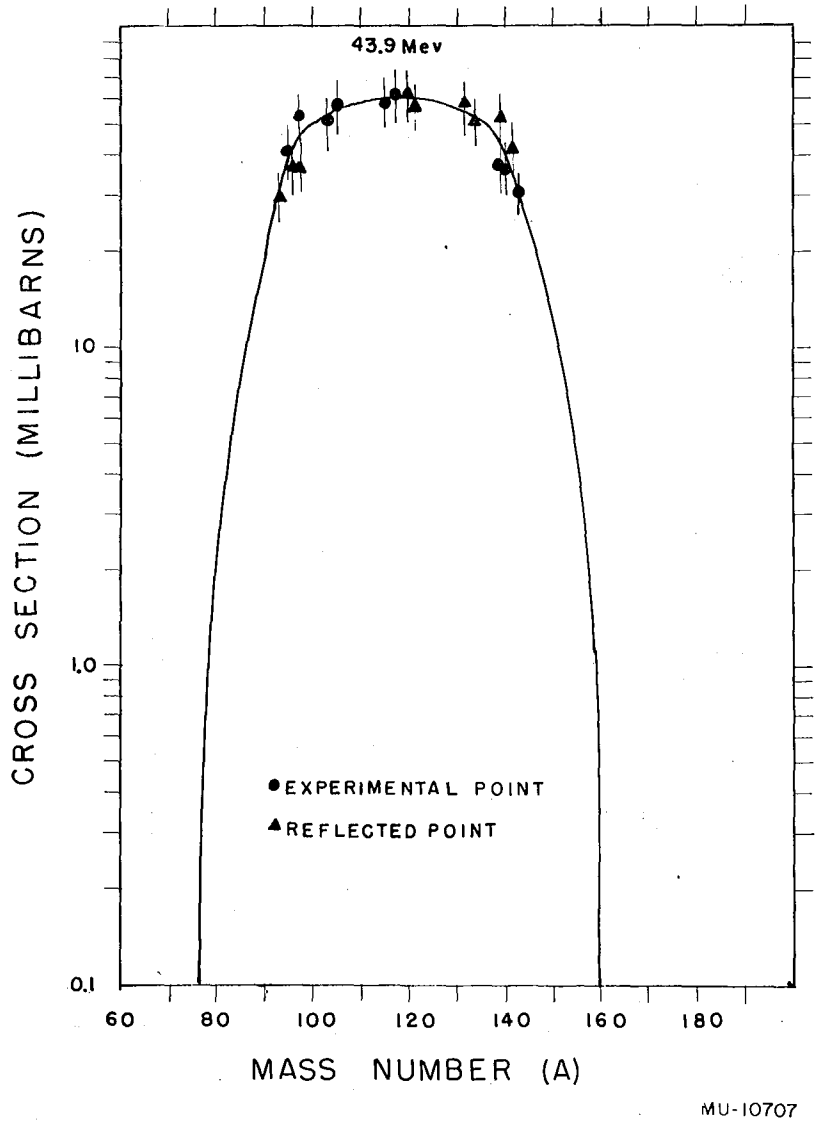

Fig. 7. Fission yield versus mass curve of the fission products formed in bombardment of U^{238} with 43.9 Mev helium ions.

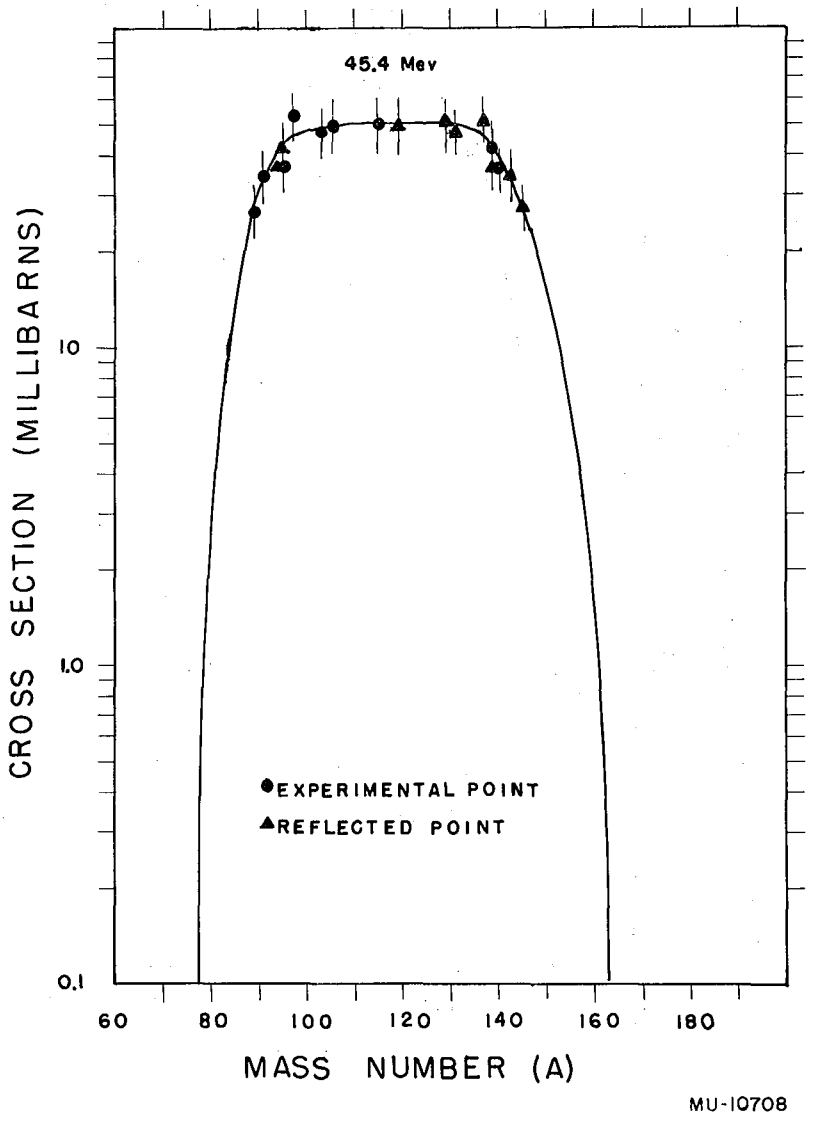

Fig. 8. Fission yield versus mass curve of the fission products formed in bombardment of U^{238} with 45.4 Mev helium ions.

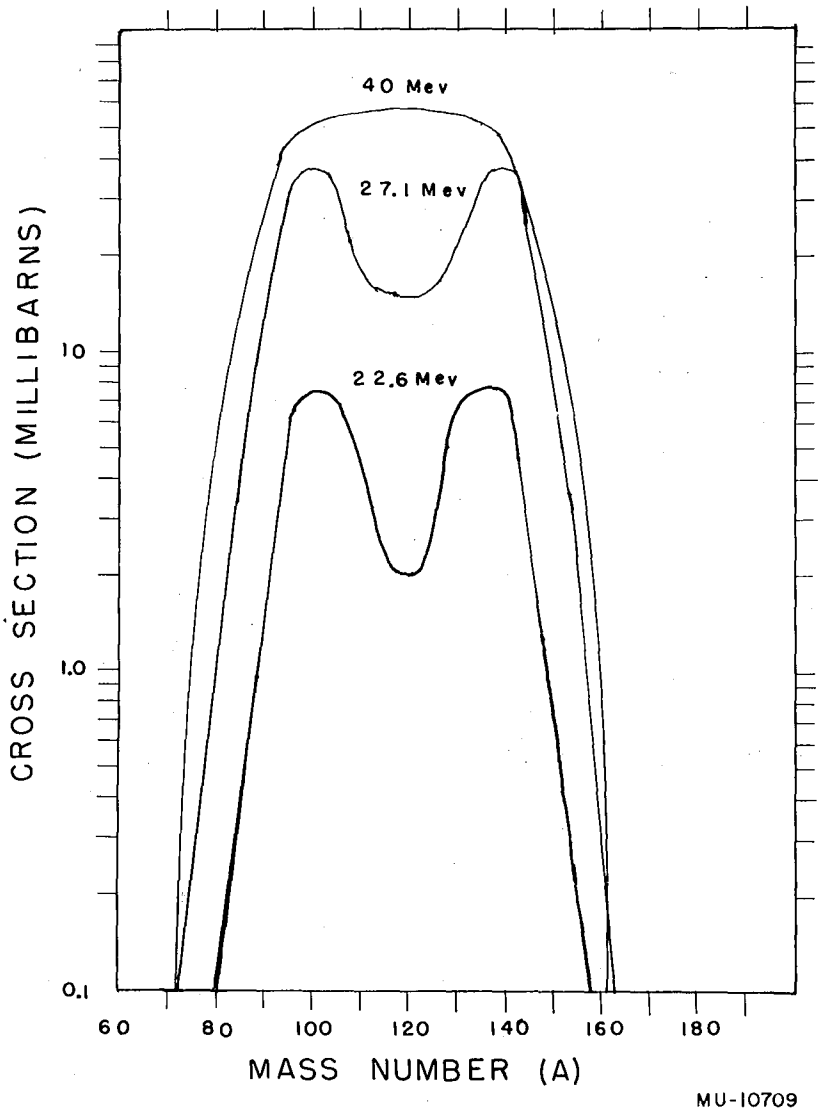

Fig. 9. Variation of fission yield curves with energy.

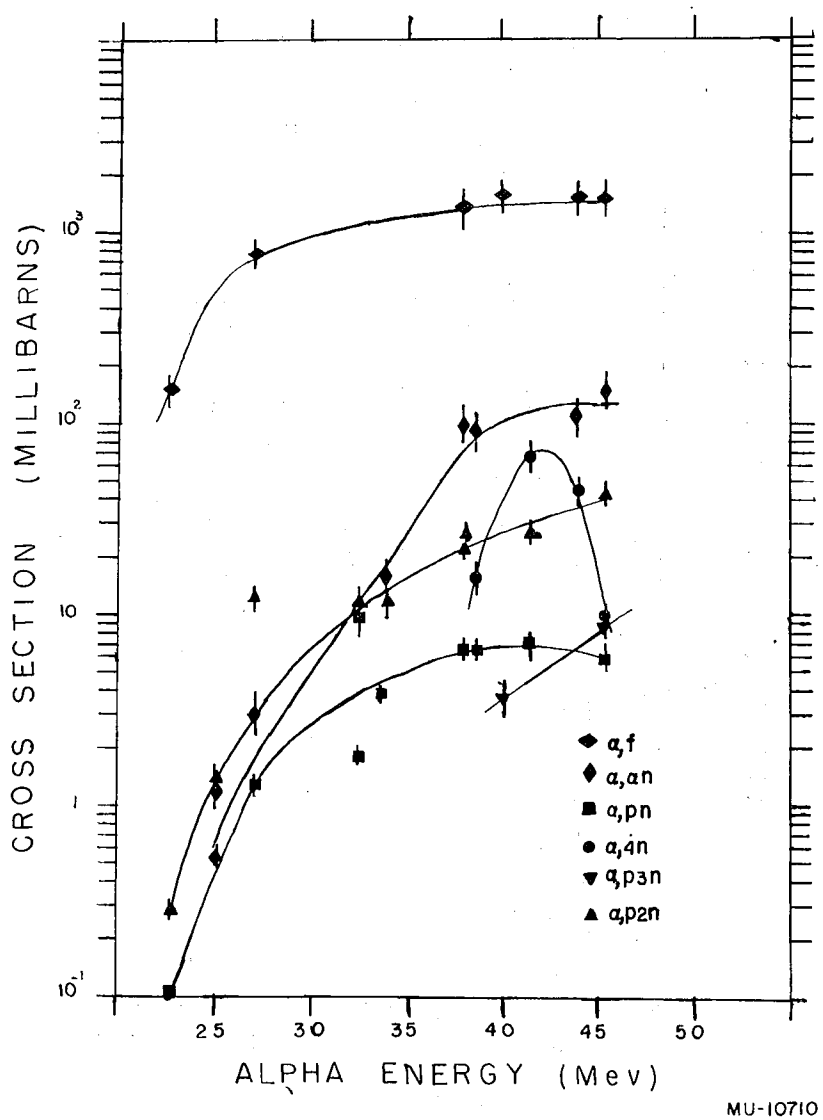

Fig. 10. Comparison of the total fission excitation curves with the spallation excitation curves.

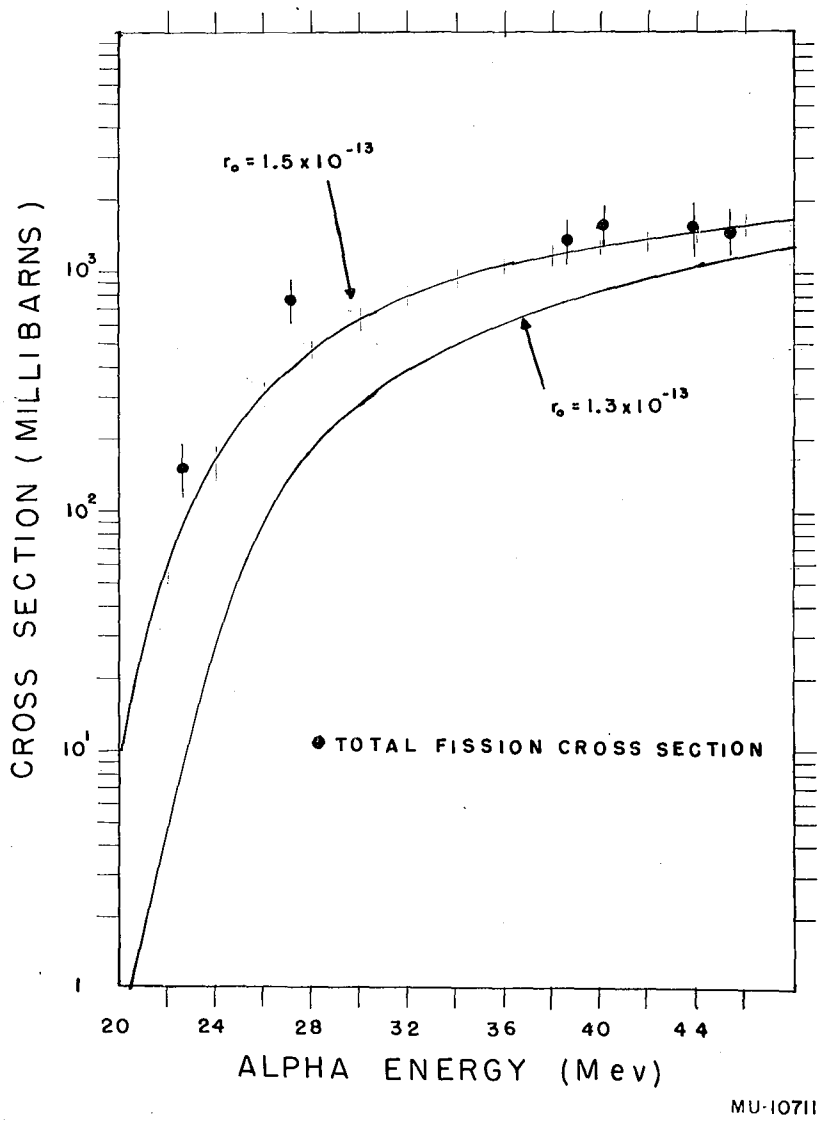

Fig. 11. Comparison of the total fission excitation function with theoretical total reaction cross section excitation functions.